RAPID COMMUNICATION

A single diffractive optical element implementing spectrum-splitting and beam-concentration functions simultaneously with high diffraction efficiency*

Ye Jia-Sheng(叶佳声)[a)b)], Wang Jin-Ze(王进泽)[c)], Huang Qing-Li(黄庆礼)[c)], Dong Bi-Zhen(董碧珍)[c)], Zhang Yan(张 岩)[a)b)†], and Yang Guo-Zhen(杨国桢)[c)‡]

[a)] *Department of Physics, Capital Normal University, Beijing* 100048, *China*

[b)] *Beijing Key Laboratory for THz Spectroscopy and Imaging, Key Laboratory of THz Optoelectronics, Ministry of Education, Beijing* 100048, *China*

[c)] *Institute of Physics, Chinese Academy of Sciences, Beijing* 100190, *China*

(Received 22 November 2012; revised manuscript received 6 December 2012)

In this paper, a novel method is proposed and employed to design a single diffractive optical element (DOE) for implementing spectrum-splitting and beam-concentration (SSBC) functions simultaneously. We develop an optimization algorithm, through which the SSBC DOE can be optimized within an arbitrary thickness range according to the limitations of modern photolithography technology. Theoretical simulation results reveal that the designed SSBC DOE has a high optical focusing efficiency. It is expected that the designed SSBC DOE should have practical applications in high-efficiency solar cell systems.

Keywords: diffractive optical element, spectrum-splitting and beam-concentration functions, thickness optimization algorithm, solar cell systems

PACS: 42.15.Eq, 42.25.Fx, 42.79.Ek **DOI:** 10.1088/1674-1056/22/3/034201

1. Introduction

Energy resources and environmental problems are common challenges that everyone in the world is facing. Solar energy, due to its cleanness and abundance, fuels the need for the future. Nowadays, the solar energy is usually utilized through the solar cells by making use of the photovoltaic (PV) effect.[1] A solar cell is composed of an optical system and a cell system. The merit of a PV cell depends on the manufacturing cost of the PV material as well as the cell's efficiency.

In order to reduce the cost, the incident sunlight is often highly concentrated to reduce the number of expensive cells used.[2] An alternative way is decreasing the fabrication difficulty by using an optical system. In this case, the sunlight is spatially separated into different regions where properly selected single junction solar cells are aligned.[3] Since cell stacking and epitaxial technologies[4] are no longer applied, it becomes much cheaper and easier.

On the other hand, for achieving a high cell efficiency, the following three main strategies are used.[5] Firstly, high efficiency converting materials such as the III–IV compounded materials are selected[6] instead of the silicon. Secondly, several junctions with different bandgaps are stacked together from top to bottom[7] to break the maximum conversion efficiency of a single bandgap converter limited by the Shockley–Read–Hall equation.[8] However, some constraints on choosing the materials and substrates exist due to the lattice matching problems. Thirdly, the cell efficiency may also be raised by using new mechanisms, new materials, and subwavelength structures, including the local light trapping techniques,[9–12] plasmonics,[13–15] organic solar cells,[16] photonic crystals,[17–19] optical waveguides,[20] and nano-patterned structures.[21–23]

On summarizing the above two aspects for achieving a high conversion efficiency and low cost, we find two critical optics issues in promoting the wide applications of solar cells. One is the spectrum-splitting problem, and the other is the beam-concentration problem. For implementing the spectrum-splitting function, three types of elements are usually applied, namely, prisms, diffraction gratings, and dichroics. For realizing the beam-concentration function, an optical lens is needed. In the previous papers, these two functions are generally realized by two elements in successive steps.[24,25] As a result, it brings problems such as system stableness, system compactness, and alignment errors. To solve the problems, in this paper we design a single diffractive optical element (DOE) that can implement spectrum-splitting and beam-concentration (SSBC) functions simultaneously. In order to make use of the modern photolithography technology in the

*Project supported by the National Basic Research Program of China (Grant No. 2011CB301801) and the National Natural Science Foundation of China (Grant Nos. 91233202, 10904099, 11204188, 61205097, and 11174211).

†Corresponding author. E-mail: yzhang@mail.cnu.edu.cn

‡Corresponding author. E-mail: yanggz@aphy.iphy.ac.cn

© 2013 Chinese Physical Society and IOP Publishing Ltd

fabrication process, an optimization algorithm is developed so that the thickness of the DOE can be confined within an arbitrary range.

This paper is organized as follows. In Section 2, the design principles of the SSBC DOE and the thickness optimization algorithm are described in detail. In Section 3, the parameters of the designed SSBC DOEs are given, and then their performances are presented with explanations. A conclusion is drawn in Section 4 with some discussion.

2. Designing a single DOE that implements SSBC functions simultaneously

2.1. Design principles of the SSBC DOE

Figure 1 depicts a schematic diagram of the proposed single SSBC DOE. The sunlight is normally incident upon the front surface of the DOE on the input plane. Due to the phase modulation of the surface-relief profile, the sunlight with different wavelengths will be separately focused at different preassigned positions on the output plane, as shown in Fig. 1. If we put proper semiconductor materials at the corresponding focal positions, the solar cell conversion efficiency is expected to be significantly raised. Then, the design of such an SSBC DOE is considered.

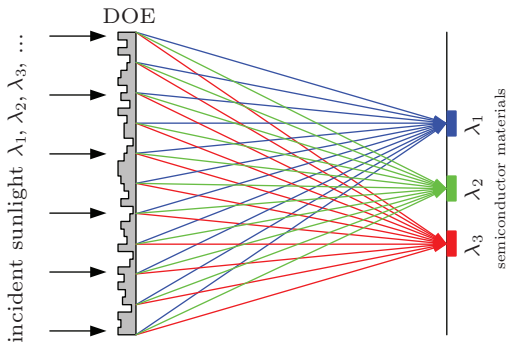


Fig. 1. Schematic diagram of a single DOE that implements SSBC functions simultaneously.

As is well known, the diffraction grating and the lens can realize spectrum-splitting and beam-concentration functions, respectively. From our experience in physical optics, if we attach these two elements together, the combined element should have both functions simultaneously, as shown in Fig. 2(a). From diffractive optics, for a definite incident wavelength λ_i, the focusing refractive lens in Fig. 2(a) has a thickness function

$$h_{\mathrm{rl}} = -x^2/\{2[n(\lambda_i)-1)]f\}, \tag{1}$$

where $n(\lambda_i)$ represents the refractive index of the lens at wavelength λ_i $(i = 1,2,3,\ldots)$; x stands for the horizontal coordinate with the origin at the center; and f denotes the preset focal length. The spectrum-splitting grating may be regarded as a Fresnel prism, as shown by the blue element in Fig. 2(a). Its thickness is given by

$$h_{\mathrm{g}} = \mathrm{mod}(px, \Delta h_0), \tag{2}$$

where $\mathrm{mod}(A,B)$ means the modulus function and its value situates within $[0,B)$ for any positive real numbers A and B; p denotes the slope of the prism; $\Delta h_0 = \lambda_0/[n(\lambda_0)-1]$, and λ_0 is chosen as the average wavelength in the considered wavelength range. Theoretically, although the combined element can fulfill the SSBC functions, it is usually too thick to fabricate because of the thick refractive lens, as shown by the red element in Fig. 2(a). Therefore, we call it a bulk SSBC DOE, whose thickness is given by

$$h_{\mathrm{b}} = h_{\mathrm{rl}} + h_{\mathrm{g}}. \tag{3}$$

In order to utilize modern photolithography technology, the thickness of the designed SSBC DOE should be confined in a reasonable range. In physical optics, as the 2π phase can be added or removed without influencing the performance of the DOE, the refractive lens may be attenuated into a Fresnel lens while the grating part is kept unchanged. For instance, at wavelength λ_1, the thickness of the combined element after attenuation is

$$h_{11}(\lambda_1) = \mathrm{mod}(h_{\mathrm{rl}}, \Delta h_1) + h_{\mathrm{g}}, \tag{4}$$

where $\Delta h_1 = \lambda_1/[n(\lambda_1)-1]$ corresponds to a phase change of 2π for wavelength λ_1, and $n(\lambda_1)$ denotes the material refractive index at wavelength λ_1. When the incident wavelength becomes λ_2, λ_3,..., we can obtain h_{12}, h_{13},..., as shown in Fig. 2(b). Then a new problem arises. For the solar cell system, as the incident sunlight includes multiple wavelengths, from Eq. (4), we cannot get a unique boundary profile for the designed SSBC DOE.

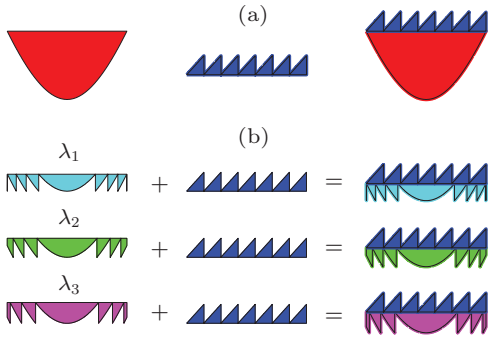


Fig. 2. Diagrams for interpreting the design principles of (a) bulk and (b) optimized SSBC DOEs.

2.2. A thickness optimization algorithm for designing the SSBC DOE

To solve the above problem, in this subsection we develop a thickness optimization algorithm. For wavelength λ_1, it has a ground thickness h_{11}. Let us assume that the largest permitted thickness of the designed DOE is $h_{\max}$, which is usually

limited by the experimental fabrication conditions. Since multiples of 2π phase do not have any impact on the DOE's performance, a series of equivalent thicknesses may be obtained as

$$h_1 = h_{11} + l\Delta h_1\,, \tag{5}$$

where $l = 0, 1, 2, \ldots$. The maximum value of l is governed by $h_1 \le h_{\max}$. Similarly, for another incident wavelength λ_2, we obtain its corresponding series of equivalent thicknesses as

$$h_2 = h_{12} + m\Delta h_2\,, \tag{6}$$

where $m = 0, 1, 2, \ldots$, $\Delta h_2 = \lambda_2/[n(\lambda_2) - 1]$, and $n(\lambda_2)$ represents the material refractive index at wavelength λ_2, as shown in Fig. 3. The maximum value of m is determined by $h_2 \le h_{\max}$.

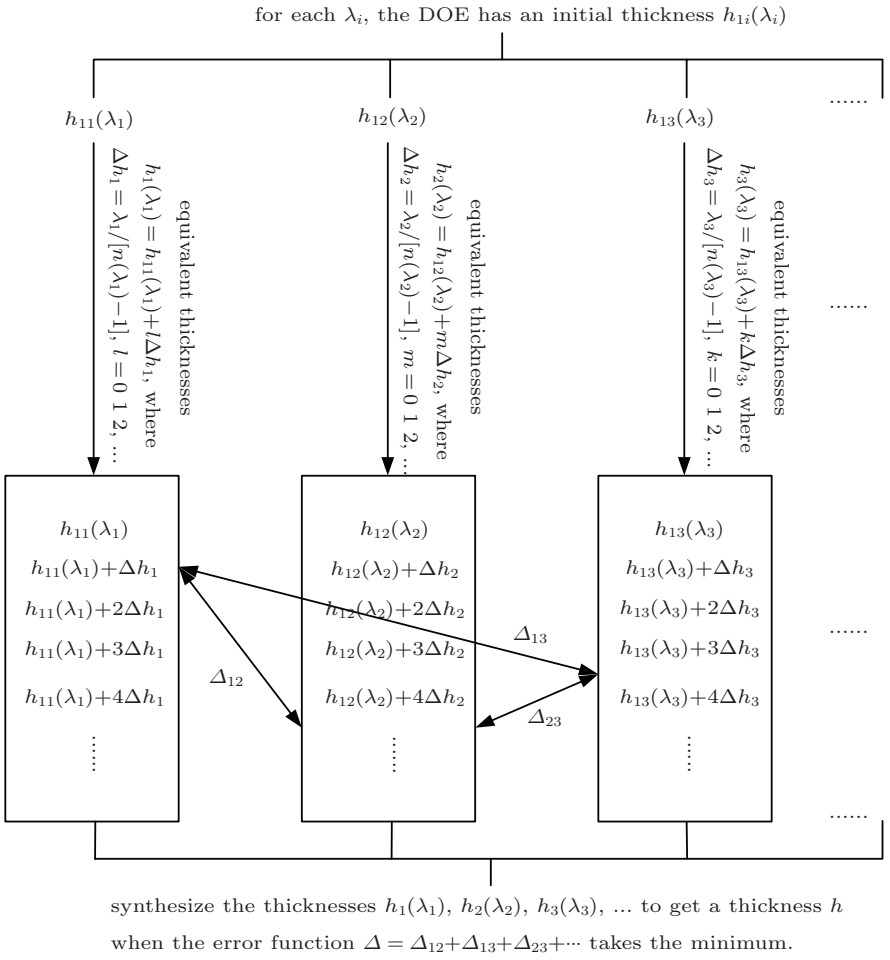


Fig. 3. Flow chart for the thickness optimization algorithm.

Following the above steps, we can generate a unique set of thicknesses for each wavelength. From each set, we arbitrarily select a thickness. If the total wavelength number is M, altogether we will have M thicknesses. The error between two arbitrary thicknesses is calculated as $\Delta_{ij} = |h_i - h_j|$. We define an error function

$$\Delta = \sum_{i=1,M}^{j=i+1,M} \Delta_{ij}. \tag{7}$$

Through searching the minimum value of Δ, the optimum thickness in each set will be determined, as shown in Fig. 3. Finally, the thickness of the SSBC DOE is optimized as

$$h = \frac{1}{M}\sum_{i=1}^{M} h_i\,. \tag{8}$$

As the thickness h in Eq. (8) may take any continuous value, in the following we refer to it as $h_{\rm c}$ $(= h)$. Since modern photolithographic fabrications are implemented through binary masks, the continuous DOEs are usually quantized into multilevel ones in the following way. If the maximum permitted thickness is $h_{\max}$ and the total quantization level number is N, each step depth is $\Delta h = h_{\max}/N$. The thickness of the quantized DOE, $h_{\rm q}$, is derived from that of the continuous one $h_{\rm c}$ as

$$h_{\rm q} = {\rm Int}(h_{\rm c}/\Delta h) \times \Delta h, \tag{9}$$

where ${\rm Int}(C)$ means taking the maximum integer to be no larger than the real number C.

3. Performance simulation results of the designed SSBC DOEs

3.1. Design parameters and performance characterization

To demonstrate the validity of the proposed method, we will design an SSBC DOE and characterize its performance. The parameters are selected as follows. The incident wavelength ranges from 0.45 μm to 0.65 μm. In the designing processes shown in Figs. 2 and 3, we choose three wavelengths, i.e., 0.45 μm, 0.55 μm, and 0.65 μm. Therefore, the wavelength number in Eq. (8) is $M = 3$. The average wavelength is $\lambda_0 = 0.55$ μm. The distance between the input and the output planes is $f = 800$ mm. We define the length unit as $l_0 = \sqrt{\lambda_0 \times f} \approx 0.6633$ mm. The grating angle is $\theta = \pi/160$, therefore, the constant p in Eq. (2) is $p = \tan(\pi/160)$. Both the input and the output planes have the same size of $32l_0 \approx 21.23$ mm. The input and the output planes are equally quantized into 4096 segments, the size of each element is about 5.18 μm. The material used is chosen as fused silica, whose refractive index changes slightly in the visible region. Hence, we neglect the dispersive effect and assume the refractive index to be a constant as $n = 1.46$.[26] Following the design procedure in Section 2, the SSBC DOE can be obtained.

After designing the DOE, under the thin-element approximation we can calculate the field distribution on the input plane (just passing through the DOE) as

$$U_1(X_1, \lambda_i) = \exp\left[\mathrm{j}\frac{2\pi(n-1)h(X_1)}{\lambda_i}\right], \tag{10}$$

where $h(X_1)$ represents the thickness of the DOE; $h(X_1)$ equals $h_c(X_1)$ or $h_q(X_1)$ for the bulk or optimized SSBC DOE, respectively; X_1 denotes the transverse coordinate of the sampling point on the input plane. It is noted that the reflection losses on both interfaces of the DOE are ignored. As the propagation distance is far enough, the Fresnel diffraction integral is applied to calculate the field on the output plane[27]

$$U_2(X_2, \lambda_i) = \int U_1(X_1, \lambda_i)\hat{G}(X_1, X_2, \lambda_i)\mathrm{d}X_1, \tag{11}$$

where X_2 represents the transverse coordinate on the output plane; and $\hat{G}$ denotes the Fresnel diffraction integral kernel given by

$$\hat{G}(X_1, X_2, \lambda_i) = \frac{1}{\sqrt{\mathrm{j}\lambda_i f}}\exp(\mathrm{j}2\pi f/\lambda_i) \times \exp[\mathrm{j}\pi(X_1 - X_2)^2/(\lambda_i f)]. \tag{12}$$

In order to characterize the performance of the DOE, the optical focusing diffraction efficiency η_i for each wavelength λ_i is defined as

$$\eta_i = \frac{\int_{x_i - l_0}^{x_i + l_0} |U_2(X_2, \lambda_i)|^2 \mathrm{d}X_2}{\int_{-\infty}^{+\infty} |U_1(X_1, \lambda_i)|^2 \mathrm{d}X_1}, \tag{13}$$

where x_i denotes the geometrical transverse focal position for wavelength λ_i; and $|U_j|$ $(j = 1, 2)$ represents the magnitude of a complex number U_j. The ultimate optical focusing diffraction efficiency of the designed SSBC DOE is averaged as

$$\eta = \frac{1}{M}\sum_{i=1}^{M}\eta_i. \tag{14}$$

3.2. Performance of the designed bulk SSBC DOE

Firstly, we design a bulk SSBC DOE which consists of a refractive lens and a diffraction grating without any thickness limitation. By following the design procedure in Subsection 2.1, the thickness of the bulk SSBC DOE is evaluated. Apparently, by ignoring the material dispersive effect, the boundary of the bulk SSBC DOE does not depend on the designing wavelength. Therefore, it suits all the designed wavelengths well and is expected to have a very good performance. Through calculating the Fresnel diffraction integral, the intensity distributions on the output plane are obtained and displayed in Fig. 4. The blue, green, and red curves correspond to the intensity distributions for incident wavelengths of 0.45 μm, 0.55 μm, and 0.65 μm, respectively. It is seen from Fig. 4 that the light is separately concentrated very well on the output plane. Numerical results reveal that the focusing diffraction efficiency reaches 87.93%. The full widths at half maximum (FWHMs) are 15.55 μm, 20.73 μm, and 25.91 μm for wavelengths of 0.45 μm, 0.55 μm, and 0.65 μm, respectively. The corresponding transverse real focal positions are −5.91 mm, −7.23 mm, and −8.54 mm. For comparison, the preset focal positions are also evaluated from the geometrical formula $x_i = -f\tan\{\arcsin[(n-1)\times\sin(\theta)]\lambda_i/\lambda_0\}$. The corresponding values are −5.91 mm, −7.23 mm, and −8.54 mm. It can be concluded that the designed bulk SSBC DOE has realized both spectrum-splitting and beam-concentration functions very well at the preassigned positions.

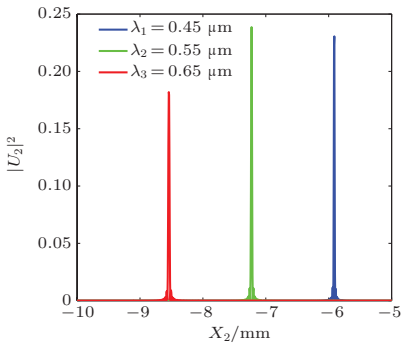


Fig. 4. Normalized intensity distributions of the designed bulk SSBC DOE on the output plane.

3.3. Performance of the optimized SSBC DOE

In Subsection 3.2, although we have successfully designed a bulk SSBC DOE with a high diffraction efficiency, the total thickness of the designed DOE is as large as 153.82 μm. In fact, such a thick element is very difficult for photolithographic fabrication with the fused silica. In this subsection,

the thickness optimization algorithm is adopted to attenuate the thickness. We have calculated the diffraction efficiencies of the optimized SSBC DOEs on varying the maximum permitted phase, as shown in Fig. 5. This phase is involved with the average wavelength, which means that a 2π-phase increase leads to a thickness increment of $\Delta h_0 = \lambda_0/(n-1) \approx 1.20$ μm. The blue curve corresponds to the optimized SSBC DOE with a continuous phase. From Fig. 5, it is obvious that the diffraction efficiency of the continuous DOE is monotonically increased as the maximum permitted phase is enlarged. With the increase of the maximum permitted phase, because we have more choices in each set of thicknesses, it becomes easier to find a thickness that satisfies all the designed wavelengths better.

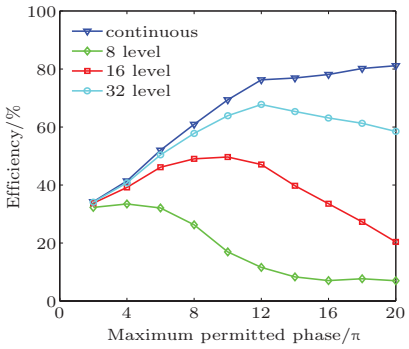


Fig. 5. Optical focusing diffraction efficiency versus the maximum permitted phase for the optimized SSBC DOEs.

Considering the practical fabrication of the optimized SSBC DOE, the continuous DOE is quantized to have a multilevel profile. The green, red, and cyan curves correspond to the 8-level, 16-level, and 32-level DOEs, respectively. For the designed multilevel DOEs, when the quantization level number is increased, the focusing diffraction efficiency is increased. This is due to the decrease of the quantization error. For a given quantization level number, there exists an optimum maximum permitted phase. It can be explained as follows. When the maximum permitted phase is too small, the selection in each thickness set is strictly limited, and thus the optimized thickness h_q deviates far from the selected thickness h_i for each wavelength. On the other hand, when the maximum permitted phase is large, it will be much easier to find an accurate thickness h_c. However, for a given quantization level number, each step depth is large, which results in a large boundary quantization error.

Figure 6(a) shows the boundary profile of the optimized 32-level SSBC DOE, which basically looks like a Fresnel lens. The inset magnifies the local part of the DOE boundary. For the optimized 32-level SSBC DOE, numerical results reveal that the optimum maximum permitted phase is 12π, corresponding to the maximum thickness of $12\pi[\lambda_0/(n-1)]/(2\pi) \approx 7.17$ μm. Under illuminating wavelengths of 0.45 μm, 0.55 μm, and 0.65 μm, the intensity distributions on the output plane are plotted in Fig. 6(b). It is clearly demonstrated that the optimized 32-level SSBC DOE has good focusing properties for all the three designed wavelengths, as most of the incident power is concentrated in the main lobe and the side lobes are suppressed well. Numerical results reveal that the average optical focusing diffraction efficiency is 67.75% for these three wavelengths. The FWHMs are 15.55 μm, 20.73 μm, and 25.91 μm for incident wavelengths of 0.45 μm, 0.55 μm, and 0.65 μm, respectively. In addition, the transverse preset and real focal positions are the same, which are −5.91 mm, −7.23 mm, and −8.54 mm.

Since sunlight has a continuous spectrum, we are curious about how the optimized 32-level SSBC DOE in Fig. 6(a) performs for other wavelengths. For this reason, we choose six incident wavelengths (475 nm, 500 nm, 525 nm, 575 nm, 600 nm, and 625 nm) to calculate the output intensities, as displayed in Fig. 6(b). For these six wavelengths, although the intensity peaks are not high, the energy concentration regions situate in turn with the increase of the incident wavelength. Even if more wavelengths are considered, we can draw a similar conclusion. In solar cell applications, we are more interested in the energy concentration position and the efficiency rather than a higher intensity peak. Numerical results reveal that the corresponding six diffraction efficiencies are 54.61%, 49.03%, 69.16%, 60.03%, 56.08%, and 70.40%. Above all, it can be concluded that the optimized 32-level DOE not only realizes the expected SSBC functions, but also has a high focusing diffraction efficiency.

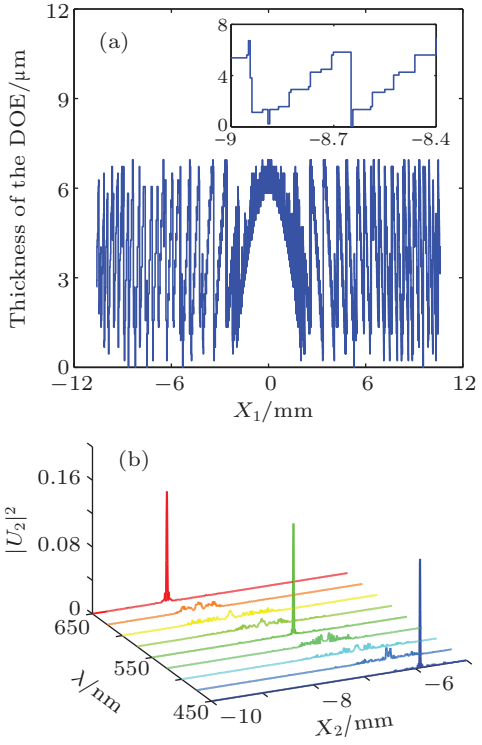


Fig. 6. (a) Boundary profile of the optimized 32-level SSBC DOE, the inset magnifies the local part of the DOE boundary. (b) Normalized output-plane intensity distributions of the optimized 32-level SSBC DOE with the maximum permitted phase of 12π.

4. Discussion and conclusion

In this paper, we propose a new method for designing the single DOE with SSBC functions. The main novelties are the following four aspects. Firstly, we present an analytical thickness formula for the bulk SSBC DOE. Secondly, a thickness optimization algorithm is developed, so the SSBC DOE can be optimized within an arbitrary thickness range. Thirdly, theoretical simulations demonstrate that the optimized SSBC DOE has a high optical focusing efficiency in the light concentration region. Lastly but not least, when the thickness of the SSBC DOE is limited in a reasonable scope, it may be fabricated by the modern photolithography technology. More importantly, if a hard mold with a complementary structure is manufactured, a mass amount of the SSBC DOEs can be duplicated by using micro imprint technology. Therefore, it probably provides a cheap way for fabricating high-efficiency solar cells.

In this paper, we just selected several wavelengths in the visible region instead of the whole solar band due to the following two reasons. One is that our main purpose is to demonstrate the validity of the proposed method, and the visible range is an important band in the solar spectrum. The other reason is that experimental verifications will be easier to carry out for visible light. Fabrications of the optimized SSBC DOE are in progress and their performance will be measured to verify our theoretical predictions.

References

[1] Razykov T M, Ferekides C S, Morel D, Stefanakos E, Ullal H S and Upadhyaya H M 2011 *Solar Energy* **85** 1580

[2] Chang L B and Shan K 2011 (US patent) 0 056 530

[3] Imenes A G and Mills D R 2004 *Sol. Energy Mater. Sol. Cells* **84** 19

[4] Kurtz S and Geisz J 2010 *Opt. Express* **18** A73

[5] Barnett A, Kirkpatrick D, Honsberg C, Moore D, Wanlass M, Emery K, Schwartz R, Carlson D, Bowden S, Aiken D, Gray A, Kurtz S, Kazmerski L, Steiner M, Gray J, Davenport T, Buelow R, Takacs L, Shatz N, Bortz1 J, Jani O, Keith Goossen K, Kiamilev F, Doolittle1 A, Ferguson I, Unger B, Greg Schmidt G, Christensen E and Salzman D 2009 *Prog. Photovolt: Res. Appl.* **17** 75

[6] Tanabe K 2009 *Energies* **2** 504

[7] Tobias I and Luque A 2002 *Prog. Photovolt: Res. Appl.* **10** 323

[8] Shockley W and Queisser H J 1961 *J. Appl. Phys.* **32** 510

[9] Rim S B, Zhao S B, Scully S R, McGehee M D and Peumans P 2007 *Appl. Phys. Lett.* **91** 243501

[10] Ferry V E, Verschuuren M A, Li H B T, Verhagen E, Walters R J, Schropp R E I, Atwater H A and Polman A 2010 *Opt. Express* **18** A237

[11] Raman A, Yu Z F and Fan S H 2011 *Opt. Express* **19** 19015

[12] Zheng G G, Jiang J L, Xian F L, Qiang H X, Wu H and Li X Y 2011 *Chin. Phys. B* **20** 094201

[13] Catchpole K R and Polman A 2008 *Opt. Express* **16** 21793

[14] Atwater H A and Polman A 2010 *Nat. Mater.* **9** 205

[15] Ren W Z, Zhang G H, Wu Y K, Ding H Y, Shen Q H, Zhang K, Li J W, Pan N and Wang X P 2011 *Opt. Express* **19** 26536

[16] Hoppe H and Sariciftci N S 2004 *J. Mater. Res.* **19** 1924

[17] Chutinan A, Kherani N P and Zukotynski S 2009 *Opt. Express* **17** 8871

[18] Park Y, Drouard E, Daif O E, Letartre X, Viktorovitch P, Fave A, Kaminski A, Lemiti M and Seassal C 2009 *Opt. Express* **17** 14312

[19] Zheng G G, Xian F L and Li X Y 2011 *Chin. Phys. Lett.* **28** 054213

[20] Rühle S, Greenwald S, Koren E and Zaban A 2008 *Opt. Express* **16** 21801

[21] Liu Y, Sun S H, Xu J, Zhao L, Sun H C, Li J, Mu W W, Xu L and Chen K J 2011 *Opt. Express* **19** A1051

[22] Jonsson G E, Fredriksson H, Sellappan R and Chakarov D 2011 *Int. J. Photoenergy* **2011** 939807

[23] Xiong B T, Zhou B X, Bai J, Zheng Q, Liu Y B, Cai W M and Cai J 2008 *Chin. Phys. B* **17** 3713

[24] Kintisch E 2007 *Science* **317** 583

[25] McCambridge J D, Steiner M A, Unger B L, Emery K A, Christensen E L, Wanlass M W, Gray A L, Takacs L, Buelow R, McCollum T A, Ashmead J W, Schmidt G R, Haas A W, Wilcox J R, Van Meter J, Gray J L, Moore D T, Barnett A M and Schwartz R J 2011 *Prog. Photovolt: Res. Appl.* **19** 352

[26] Bass M, Stryland E W V, Williams D R and Wolfe W L 1995 *Handbook of Optics, Volume II, Devices, Measurements, and Properties* (2nd edn.) (New York: McGraw-Hill Press)

[27] Goodman J W 1968 *Introduction to Fourier Optics* (San Francisco: McGraw-Hill Press) Chaps. 3, 4